

University of Nevada, Reno

**Au@Pt Core-Shell Nanoparticles as Solid Contacts in Ion Selective  
Electrodes for Ammonium Detection**

A thesis submitted in partial fulfillment of the  
requirements for the degree of Master of Science in  
Biomedical Engineering

by

Masoumeh Saber Zaeimian

Xiaoshan Zhu, Ph.D., Advisor

May 2019



THE GRADUATE SCHOOL

We recommend that the thesis  
prepared under our supervision by

**MASOUMEH SABER ZAEIMIAN**

Entitled

**Au@Pt Core-Shell Nanoparticles as Solid Contacts in  
Ion Selective Electrodes for Ammonium Detection**

be accepted in partial fulfillment of the  
requirements for the degree of

MASTER OF SCIENCE

Xiaoshan Zhu, Ph.D, Advisor

Hao Xu, Ph.D, Committee Member

Yu Yang, Ph.D, Graduate School Representative

David W. Zeh, Ph.D., Dean, Graduate School

May, 2019

## **Abstract**

In this thesis, we present a novel ion selective electrode for ammonium detection in human perspiration. Ion selective electrodes provide the sensing capability to measure a specific ion in a sample. This makes them applicable in many areas, such as environmental monitoring, clinical analysis, and process control. The proposed ion-selective electrode contains solid contact instead of internal solutions as is the case for conventional ion selective electrodes. This property of the proposed electrode makes it smaller and maintenance-free.

So far, different kinds of material have been used as solid contacts in ion selective electrodes. In this work, we propose the use of gold (Au) and Platinum (Pt) for the solid contact of the ion selective electrode. Since, Au@Pt core-shell nanoparticles exhibit simple particle synthesis, high stability, and large surface of particle for high electrochemical activities, using them as a transducer section in an ion selective electrode for ammonium detection is proposed in this work. To this end, we synthesized these two elements as nanoparticles with a core-shell structure. The core is made of Au and Pt forms the surrounding dendritic shell with high surface area. The utilized approach reduces the complexity of Au@Pt synthesis to one step of synthesis and helps in consuming less Platinum.

Finally, the test results for different ISE configurations and various concentrations of ammonium solutions show that the proposed method has good response time and stability

characteristics compared to other configurations. Furthermore, selectivity, light and pH test results demonstrated suitability of the proposed ion selective electrode for real-world applications.

## **Acknowledgements**

I would like to express my sincere gratitude to my supportive advisor Dr. Xiaoshan Zhu for providing a constructive and friendly atmosphere for my progress. His guidance and expert advice have been invaluable throughout all stages of this work. I would also wish to express my acknowledgement to my advisory committee members, Dr. Hao Xu and Dr. Yu Yang. My special thanks go to my friend and my husband, Pourya, who helped me in every aspect to overcome the obstacles I encountered during my graduate studies. I am also always grateful to my beloved parents.

The thesis has also benefited from comments and suggestions made by Professor Konstantin Mikhelson, who gave me valuable advices and helpful information.

I also would like to thank members of our group at Integrated Bio-analytical Systems Laboratory, Brandon Gallian, Siqi Chen, Violeta Demillo, and Anthony V Piazza for providing a pleasant and friendly atmosphere.

## Table of Contents

Chapter 1 : Introduction .....	1
1-1- Au@Pt Core-Shell Nanoparticles .....	1
1-2- Metal Nanoparticles and Nanoalloys Synthesis .....	4
1-2-1- Au@Pt Synthesis .....	5
1-3- Particle Characteristics and Measurement Methods .....	7
1-3-1- Electron Microscopy .....	7
1-3-2- X-ray Spectroscopy .....	8
1-4- Nanoalloys Applications .....	8
1-5- Ion Selective Electrode .....	9
1-5-1- Ionophore-Based Membrane ISEs .....	10
1-5-2- Polymers and Plasticizers in ISE Membranes .....	11
1-5-3- Ion Selective Electrode Characteristics .....	12
1-5-4- ISEs Applications .....	14
1-6- Overview of the thesis .....	15
Chapter 2 : Au@Pt Core-Shell Nanoparticles Synthesis and Characteristics .....	18

2-1-	Introduction .....	18
2-2-	Other Published Works .....	20
2-3-	Au@Pt Core-Shell Nanoparticles .....	21
2-3-1-	Material and Equipment .....	21
2-3-2-	Au@Pt Core-Shell Nanoparticles Synthesis .....	22
2-3-3-	Washing and Drying the Synthesized Particles .....	23
2-4-	Conclusion.....	27
 Chapter 3 : Au@Pt Core-Shell Nanoparticles as Solid Contacts in Ion Selective Electrodes for Ammonium Detection .....		
3-1-	Introduction .....	30
3-2-	Other Published Works .....	31
3-3-	Experimental Methods .....	32
3-3-1-	Chemicals and Apparatus.....	32
3-3-2-	Ion Selective Membrane Preparation and ISE Fabrication .....	33
3-3-3-	Artificial Sweat Preparation .....	35
3-3-4-	Selectivity Test Procedure and Potentiometric Selectivity Coefficient .....	35
3-3-5-	pH Adjustment.....	36

3-4- Test Results .....	36
3-5- Conclusion.....	48
Chapter 4 : Conclusion.....	52
4-1- Conclusion.....	52
4-2- Future Work.....	53

**List of Tables**

Table 3-1: Sensing performance of the three ISE configurations.....41

Table 3-2: Sensing performance comparison with other reported electrodes. ....42

## List of Figures

Figure 1-1: Types of chemical mixing patterns for nanoalloys. ....	2
Figure 1-2: Structures of core-shell bimetallic nanoparticles.....	3
Figure 1-3: The general schematic of Au@Pt core-shell NP .....	6
Figure 2-1: Au@Pt synthesis at different reaction times. ....	23
Figure 2-2: Washing procedure of the synthesized Au@Pt. ....	24
Figure 2-3: TEM images of Au@Pt core-shell NPs .....	25
Figure 2-4: EDX results of Au@Pt particles.....	26
Figure 3-1: The scheme of the ion selective electrode (ISE) for ammonium detection..	34
Figure 3-2: Three configurations of the ISE.....	37
Figure 3-3: The calibration curves of the ISEs.....	38
Figure 3-4: The electrode responses of the ISEs versus time.....	39
Figure 3-5: The water layer tests on the ISEs.....	40
Figure 3-6: Effect of pH values on the response of the proposed electrode.....	43
Figure 3-7: Effect of light on the response of the proposed electrode.....	43
Figure 3-8: The repeatability testing results of three fabricated electrodes .....	45

Figure 3-9: The measurement stability of three fabricated electrodes .....46

Figure 3-10: A representative real-world measurement of the artificial sweat .....47

## **Chapter 1 : Introduction**

### **1-1- Au@Pt Core-Shell Nanoparticles**

Nanomaterials and nanoparticles (NPs) have one or more dimensions in less than 100 nanometer range, which show novel properties from their bulk materials [1]. A wide variety of nanoparticles are based on metallic elements. A single metallic element or more than one metal can form metal nanoparticles. The desire to fabricate materials with well-defined, controllable properties, and structures, on the nanometer scale, coupled with the flexibility by intermetallic materials, has generated interest in bimetallic and multi-metallic nanoalloys. Chemical reactivity and catalytic activity of nanoalloys are determined by surface structures, compositions and segregation properties of them [1]. Bimetallic nanoalloys can be different in characteristics by reasonably varying the composition and size of the constituent materials.

Due to potential unique optical, electronic, catalytic or photocatalytic properties that are absent in the monometallic nanoparticles, bimetallic composite nanoparticles attract more attention than monometallic nanoparticles from both scientific and technological viewpoints. Bimetallic nanoparticles (BNPs) not only present the properties related to the two constructing individual metals, but also may exhibit new properties due to interaction between the two metals. The distribution modes of the two metals define the structure of bimetallic nanoparticles [2]. Four main types of chemical mixing pattern can be identified for nanoalloys. As Figure 1-1 shows they are core-shell, layered segregated, mixed, and multishell nanoalloys [1]. The fabrication methods characterize the shape and size of

mono and bimetallic nanoparticles. They condition and affect the physicochemical properties of resulted final nanomaterial [2].

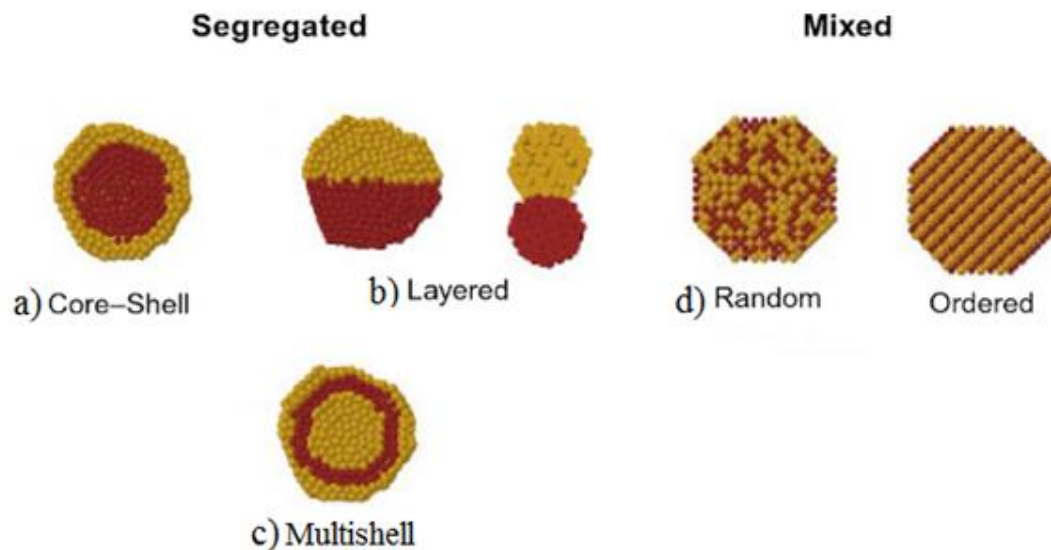


Figure 1-1: Types of chemical mixing patterns for nanoalloys [1-3].

Core-shell nanostructures consist of a shell made of one type of metal atoms surrounding a core made of another metal. Different categories of core-shell structures are shown in Figure 1-2. The core-shell structure's ability to tune the activity of the shell metal through interactions with the core has proved it as an attractive catalytic component [4].

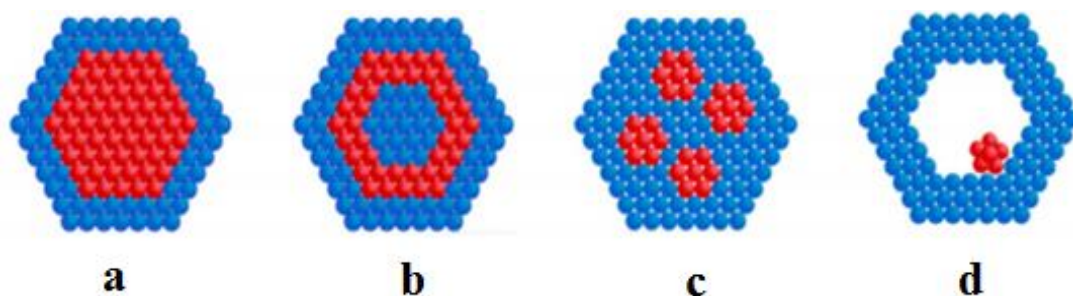


Figure 1-2: Structures of core-shell bimetallic nanoparticles: (a) Core-shell nanoparticles; (b) Multi-shell nanoparticles; (c) Multiple small core material coated by a single shell material, (d) Movable core within a hollow shell material [5-6].

In this work the core-shell category was chosen for Au@Pt nanoparticles preparation due to the large particle surface and simple synthesis procedure. The advantage of using Au NPs as template to design Au@Pt core shell NPs include the self-assembly, stability and the ability to prepare monodispersed colloids with a wide diameter range (1.5 to 100 nm) [7]. Au@Pt NPs are preferable due to their long-term stability and simple and versatile synthetic approaches [8].

The core-shell construction of synthesized Au@Pt in this work is the same as the structure in Figure 1-1.a and Figure 1-2.a. Bimetallic core-shell nanospheres with a Pt shell have been widely studied in the literature. In comparison to homogeneous Pt structures, such core-shell nanostructures not only improve the utilization efficiency of catalysts, but also decrease Pt consumption in catalysts and make it more economically feasible. In order to reduce the synthesis difficulty of core-shell nanospheres with a Pt shell and adjust the Pt shell thickness in bimetallic core-shell structure, bimetallic Au@Pt

nano-colloids with an Au core and a dendritic Pt shell were used by utilizing a surfactant-assisted process with an ultrasonic irradiation procedure [9].

The reduction process is based on transfer of electron from reducing agent (electron donor) to the metal ions (electron recipient). In many cases, core-shell structures are made through subsequent reduction of first metal to form a core followed by reduction of second metal ions to coat it [2].

### **1-2- Metal Nanoparticles and Nanoalloys Synthesis**

Metal nanoparticles and nanoalloys can be generated in a variety of ambiances like solution, gas phase, supported on a substrate, embedded in a matrix or in a bacterial cell. The first method to generate nanoparticles uses cluster molecular beams by generating the metal atoms in vapor phase from a metal target.

The second technique is reduction of metal salts. In this method, chemical reduction of solution of the metal salts in the presence of surfactant ligands creates colloidal metal nanoparticles. This way passivates the nanoparticle surface and prevents too rapid aggregation. The reduction process can be done electrochemically, radiolytically, or biosynthetically. In all these cases, nanoalloys can be produced by either co-reduction or consecutive reduction of solutions of salts of the component metals [1]. The Au@Pt core-shell nanoparticles in this work was synthesized sonochemically.

The third technique for metal nanoparticles and nanoalloys synthesis is decomposition of metal complexes. To synthesize a variety of metal nanoparticles, thermal and photolytic decomposition of low valent transition metal complexes has been used. Nanoalloys can be generated by decomposing bimetallic precursor molecules or mixtures of monometallic precursors [1]. The last method for nanoalloys synthesis is ion implantation that uses ion beams with energies of approximately 100 keV to implant metal ions into bulk insulator [1].

### **1-2-1- Au@Pt Synthesis**

For Au@Pt core-shell NPs synthesis in this work, the molar ratio of Pt/Au was chosen 1.0, therefore, to hold the same ratio, 20 mM  $\text{H}_2\text{PtCl}_6$  and 20mM  $\text{HAuCl}_4$  solution were mixed with Pluronic F127 as a structural-directing agent. Pluronic surfactants such as F127 is critical for the formation of the dendritic Pt around the Au core [10-11]. After that, 0.1 M ascorbic acid (AA) solution was added, and the mixture was then sonicated. Ascorbic acid (AA), acts as a reducing agent in this synthesis. Immediately after adding the AA solution and applying ultrasonic irradiation, the color of the solution slowly changes to red-brown that shows the Au species are preferentially reduced to Au nanoparticles [9]. The reduction process for this synthesis is in the following chemical processes (1-1 to 1-3).





After 24 hours of reaction, all the dissolved metal sources are completely deposited. Finally, the color of the solution is changed to dark brown-black that displays the formation of Au@Pt core-shell NPs. The general schematic of Au@Pt core-shell NP formation is shown in the Figure 1-3.

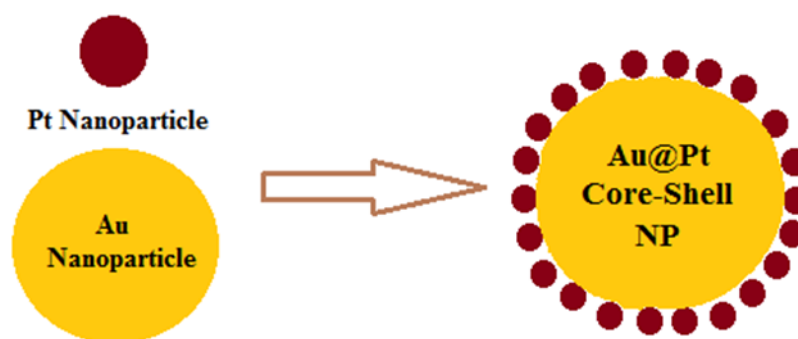


Figure 1-3: The general schematic of Au@Pt core-shell NP

The product is collected by centrifugation and residual Pluronic F127 is removed by three consecutive washing and centrifugation cycles with acetone and water. The collected product is then dried at room temperature for 2-3 days.

### **1-3- Particle Characteristics and Measurement Methods**

A variety of experimental techniques have been used to characterize and measure the properties of metal nanoparticles and nanoalloys such as mass spectroscopy, diffraction techniques, microscopy, X-ray spectroscopy, measurements of Magnetism and polarizability, ion scattering, electrochemistry, and ion mobility measurements [1]. Among them we chose transmission electron microscopy (TEM) and energy dispersive X-ray spectroscopy (EDX) for Au@Pt nanoparticles identification in our work. These two methods are explained in the following.

#### **1-3-1- Electron Microscopy**

It is important to know the degree of aggregation, size, size distribution and morphology of nanoparticles deposited or adsorbed onto a substrate. Electron microscopy is particularly useful for studying metal nanoparticles, since the electron beam can be focused down to very small dimensions. There are two types of electron microscopy, namely, transmission electron microscopy (TEM) and scanning transmission electron microscopy (STEM).

TEM is done by passing the electrons through the sample. It usually requires the nanoparticles to be dispersed onto an electron-transparent substrate, such as a thin carbon-coated microgrid. TEM has the advantage of high contrast between the metal atoms and any passivating organic molecules or polymer [1].

### **1-3-2- X-ray Spectroscopy**

Since the binding energies of the atomic core electrons are sensitive to the atomic number of the element, high energy X-ray radiation is useful for studying metal nanoparticles. It allows metals adjacent in the periodic table to be distinguished from each other. Different types of X-ray spectroscopy are X-ray absorption, X-ray photoelectron, auger electron, and energy-dispersive X-ray microanalysis spectroscopy.

In energy-disperse X-ray spectroscopy (EDX) an electron beam of between 10 keV to 20 keV is emitted on the surface of a conducting sample. This causes X-ray to be emitted, with energies depending on the material under examination. The image of the distribution of each element in the sample is obtained after scanning the electron beam across the sample. EDX produces high-resolution images, with about 1.5 nm lateral resolution, which allows spatially resolved determination of the chemical composition of individual metal nanoparticles [1].

Transmission electron microscope (TEM) and energy-dispersive X-ray (EDX) spectrometer EDX are used in our work to demonstrate the shape, size, and the composition of the synthesized particles.

### **1-4- Nanoalloys Applications**

Many of applications of metal nanoparticles is in biomedical applications, including bio-diagnostics, imaging, drug delivery, and other therapeutic applications. The combination

of the size of metal nanoparticles and the possibility of modifying their surface by coordinating surfactants to increase their lipophilicity or hydrophilicity, or to target specific cells, makes them particularly attractive in medical applications. Silver nanoparticles are now commonly used in wound dressing and in other disinfectant and antiseptic applications due to the increase in antibiotic resistant bacteria [1]. Nanoparticles are also used in clothes and footwear to kill odor-causing bacteria. There are lots of applications of nanoparticles in creating biosensors. Metal nanoparticles offer the possibility of enhanced sensitivity and selectivity over other materials. Because of their tunability, bimetallic nanoalloys show particular promise as bio-diagnostic agents [1]. Therefore, in this work the synthesized Au@Pt nanoparticles are used as a solid contact part in an ion selective electrode to detect the ammonium in human sweat.

### **1-5- Ion Selective Electrode**

Electrochemical sensors are meant to sense the presence of chemical compounds in their input chemical compositions. Their test samples can be gaseous, liquid, or even semi-solid. On the other hand, their output can be electrical current, voltage, or capacitance. A significant group of electrochemical sensors is ion-selective electrodes. The potential of an electrode follows the equation (1-4), known as the Nernst equation [12]:

$$E = E^0 + \frac{RT}{z_1 F} \ln a_I \quad (1-4)$$

In the Nernst equation  $E$  is the electrode potential,  $E^0$  is the so-called standard value of the potential,  $a_1$  is the activity and  $z_1$  is the charge number of the target analyte,  $R$  is the gas constant,  $T$  is the absolute temperature, and  $F$  is the Faraday constant. The electrode gains its standard potential value when  $a_1 = 1$  [12].

### **1-5-1- Ionophore-Based Membrane ISEs**

The membranes of ion-selective electrodes have the responsibility of separating either the internal solution or the internal solid contact of the electrode from the sample solution. It also should be selective in letting the intended types of ions to bind to it. In this way, the internal solution or solid contact would be able to respond to the proper input ions. We chose the ionophore based membrane for the proposed ammonium ion selective electrode.

Ionophores are organic lipophilic substances which selectively bind ions. Most of the time ionophores are used to detect ions selectively. However, in some cases they are used for neutral targets. The main components of ionophore membranes are solvent-polymeric membranes with polymeric matrixes that normally contain plasticizers, doped with ionophores and ion-exchangers [12]. This combination is also used in our work.

Ionophores and ion-exchangers in the electrode membrane also determine the type of the electrode response (cationic or anionic) and the selectivity of the electrode. Ionophores for solvent polymeric membranes can be categorized into two types: neutral ionophores (neutral carriers, neutral ligands) and charged ionophores (charged carriers, charged ligands) [13]. In our work we have used neutral ionophore-based membrane. Neutral

ionophores are non-electrolytes, and are nonionic species which are neither intrinsically charged, nor dissociate producing charged species. Neutral ionophores are capable of selective binding of ions with formation of ion to ionophore complexes. They are highly lipophilic molecules. Nonactin is a widely used neutral ionophore used for ammonium electrodes. It is, therefore, employed in our proposed ammonium ion-selective electrode. Since neutral ionophores, unlike ion-exchangers and charged ionophores, add no ion-exchange capacity to membranes they must be doped with ion-exchangers in ionophore-based membranes [12].

#### **1-5-2- Polymers and Plasticizers in ISE Membranes**

There are three types of membranes for ion-selective electrodes. They are glass, crystalline, and polymeric ISE membranes. Membranes made of glass are mostly used for electrodes for pH measurements and are made of silicate glasses. Crystalline electrodes can be subdivided into those with polycrystalline and with monocrystalline membranes [12]. On the other hand, ISEs with polymeric membranes containing ionophores are the most common in producing electrodes.

The percentage of ionophores in ISE membranes is commonly between 0.5% to 2% of the entire membrane mass. The rest of the membrane mass contains polymer and normally plasticizer. Polyvinylchloride is the most popular polymer among those used in ionophore-based membranes. The polymers in the ISE membrane must be mechanically robust as well as elastic. These features can be obtained by either a plasticizer added or

intrinsically low glass transition temperature ( $T_g$ ) of the polymer itself. Polymers must be stable within a reasonable temperature range, must not lose their molecular mass spontaneously, must be non-soluble in water, and stable against hydrolysis, at least up to pH 8-9 [12]. The aforementioned requirements can be achieved by adding plasticizers to poly(vinylchloride) (PVC) membranes. At temperatures below  $T_g$ , plasticizers increase elasticity of membranes and provide enough mobility of ionophores and ions within the membrane phase. Moreover, plasticizers help in dissolving ionophores in the membranes. Well-known plasticizers to be used with PVC membranes are bis(butylpentyl)adipate (BBPA), bis (2 ethylhexyl) sebacate (DOS), or 2-nitrophenyloctyl ether (o-NPOE) [12]. In our proposed ion-selective electrode, we employed o-NPOE as the plasticizer and polyvinylchloride as the polymer in the membrane.

### **1-5-3- Ion Selective Electrode Characteristics**

It is very important to test any developed ion-selective electrode for its behavioral characteristics. The functional properties of ISEs can be the working range and the response slope of the sensor, their selectivity, response time, stability of these characteristics over time, and their reproducibility from one electrode to another identically manufactured one. In the following, we explain each of the above-mentioned characteristics of an ISE.

### **1-5-3-1- Working Range and Response Slope**

The working range and response slope of the ISEs are determined directly from the calibration curve. Particularly, the lower and the upper detection limits of the ISE in the calibration curve determine its working range. The properties of the electrolyte, i.e. the nature of the anion for a cation-selective electrode and the nature of the cation for an anion-selective electrode, are the defining factors for the working range of an ISE [12].

### **1-5-3-2- Potentiometric Selectivity Coefficient**

An ideal ISE responds only to one type of target ions in a mixed sample. Nevertheless, this does not happen in real world situations. The selectivity coefficient is calculated by the activity of the target ion, charge and potentials of the target and the interfering ions. The equation for selectivity coefficient will be discussed thoroughly in Chapter 3.

Smaller selectivity coefficient value means that the interference effect caused by interfering ions is smaller and the ISE is closer to the ideal case. It means only primary ions give impact to the electrode response. For an ideally selective electrode, the output potential is constant at a constant activity of the analyte, but not necessarily at a constant concentration [12].

### **1-5-3-3- Response Time**

Response time of an ISE demonstrates the speed of the ion-selective electrode in reaching to a steady-state value of its output signal when a sample is replaced with another.

This characteristic is of great importance, because it shows how fast the sensor is able to respond to a new sample.

#### **1-5-3-4- Stability of the ISE Response**

Drift of an ISE readings immersed in the same sample over time suggest that either the standard potential ( $E^0$ ) or the slope ( $S$ ) obtained during the calibration cannot be used for measurements anymore. Typically, the standard potential is much more instable over time than the slope. The slope change is mostly due to slow leaching of ionophores from membrane to aqueous solutions [14].

The solid-contact electrodes, those without internal filling, intrinsically, are better suited for high stability of the standard potential over time. In fact, the solid-contact ISEs with glass and crystalline membranes show excellent stability over time [12]. However, for ISEs with ionophore-based membranes securing a good stability of the  $E^0$  remains a challenging task [15-16].

#### **1-5-4- ISEs Applications**

Analysis with ISEs does not require pretreatment of the samples. In addition, it makes it possible for continuous monitoring in various applications. Ion-selective electrodes and their accompanying electrical sensory instrumentation are inexpensive and easy to use, which do not necessitate high-skilled operators. From another point of view, the power consumption of ISEs is low. This makes them suitable for mobile and wearable

applications. Working as a wearable sensor needs to meet some properties like small volume detection, fast sensor response, and acceptable selectivity while the other ions exist in the sample. Among the different applications of ISEs, we may mention their application in clinical analysis, agriculture, pharmaceutical industry, food industry, environmental monitoring, industrial manufacturing, etc.

### **1-6- Overview of the thesis**

In Chapter 1, we discussed the basics of Au@Pt core-shell nanoparticle and the solid contact ISE with the Au@Pt particles as its solid contact to detect the ammonium in human sweat. The different stages of synthesis and preparation process of Au@Pt core-shell nanoparticles and the general procedure of solid contact ISE preparation were considered during this chapter. Moreover, the characteristics of each part was discussed and explained.

Chapter 1 focused on a comprehensive view of the particle and the ion selective electrode which are proposed in this thesis. Chapter 2 will mainly discuss the Au@Pt core-shell nanoparticles synthesis and the obtained practical characteristics. Chapter 3 will present the solid contact ISE with ammonium selective membrane and the electrode test results. In that chapter we discuss the fabrication of solid contact ion selective electrode to detect the ammonium in sweat. Finally, Chapter 4 concludes the work with a discussion of the final results of the proposed ISE.

## References

- [1] Richard E. Plamer. (2012) Metal Nanoparticles and Nanoalloys. Frontiers of Nanoscience Series Editor. Volume 3. Edited by Roy L. Johnston, Jess Wilcoxon. Amsterdam Netherland.
- [2] Adriana Zaleska-Medynska, Martyna Marchelek, Magdalena Diak, Ewelina Grabowska. (2016) Noble Metal-Based Bimetallic Nanoparticles: The Effect of the Structure on the Optical, Catalytic and Photocatalytic Properties. Advances in Colloid and Interface Science. Volume 229, 80–107. <https://doi.org/10.1016/j.cis.2015.12.008>.
- [3] Riccardo Ferrando, Julius Jellinek, and Roy L. Johnston. (2008) Nanoalloys: From Theory to Applications of Alloy Clusters and Nanoparticles. Volume 108, 845-910.
- [4] Selim Alayoglu, Peter Zavalij, Bryan Eichhorn, Qi Wang, Anatoly I. Frenkel, and Peter Chupas. (2009) Structural and Architectural Evaluation of Bimetallic Nanoparticles: A Case Study of Pt-Ru Core-Shell and Alloy Nanoparticles. *Acs Nano*. Volume 3, 3127–3137.
- [5] Trungdang-Bao, Danielpla, Isabellefavier, and montserratgómez. (2017) Bimetallic nanoparticles in alternative solvents for catalytic purposes *Catalysts* Volume 7. [Doi:10.3390/Catal7070207](https://doi.org/10.3390/Catal7070207)
- [6] Rajib Ghosh Chaudhuri and Santanu Paria. (2011) Core/Shell Nanoparticles: Classes, Properties, Synthesis Mechanisms, Characterization, and Applications. *Chemical Reviews*. Volume 112, 2373–2433.
- [7] Junfeng Zhai, Minghua Huang, Shaojun Dong. (2006) Electrochemical Designing of Au/Pt Core Shell Nanoparticles As nanostructured Catalyst with Tunable Activity for Oxygen Reduction. *Electroanalysis*. Volume 19, 506 - 509. [Doi: 10.1002/elan.200603728](https://doi.org/10.1002/elan.200603728).
- [8] Mei-Yun Duan, Ren Liang, Na Tian, Yong-Jun Li, Edward S. Yeung. (2013) Self-Assembly of Au-Pt Core-Shell Nanoparticles for Effective Enhancement of Methanol Electrooxidation. *Electrochimica Acta*. Volume 87, 432–437. [Http://Dx.Doi.Org/10.1016/j.electacta.2012.09.076](http://dx.doi.org/10.1016/j.electacta.2012.09.076).

[9] Hamed Atae-Esfahani, Liang Wang, Yoshihiro Nemoto, and Yusuke Yamauchi. (2010) Synthesis of Bimetallic Au@Pt Nanoparticles with Au Core and Nanostructured Pt Shell toward Highly Active Electrocatalysts. *Chem. Mater.* Volume 22, 6310–6318. Doi: 10.1021/Cm102074w.

[10] Liang Wang, And Yusuke Yamauchi. (2009) Block Copolymer Mediated Synthesis of Dendritic Platinum Nanoparticles. *J. Am. Chem. Soc.* Volume 131, 9152–9153.

[11] Liang Wang, Hongjing Wang, Yoshihiro Nemoto, and Yusuke Yamauchi. (2010) Rapid and Efficient Synthesis of Platinum Nanodendrites with High Surface Area by Chemical Reduction with Formic Acid. *Chem. Mater.* Volume, 22, 2835–2841. Doi: 10.1021/Cm9038889.

[12] Konstantin N. Mikhelson. (2013) *Ion-Selective Electrodes*. Springer-Verlag Berlin Heidelberg. Volume 81. DOI:10.1007/978-3-642-36886-8

[13] Eric Bakker, Philippe Bühlmann, and Erno Pretsch. (1997) Carrier-Based Ion-Selective Electrodes and Bulk Optodes. 1. General Characteristics. *Chem. Rev.* Volume 97, 3083–3132.

[14] Philippe Bühlmann and Yoshio Umezawa. (2000) Lifetime of Ion-Selective Electrodes Based on Charged Ionophores. *Anal. Chem.* Volume 72, 1843-1852.

[15] N. M. Ivanova, M. B. Levin, and K. N. Mikhelson. (2012) Problems and Prospects of Solid Contact Ion-Selective Electrodes with Ionophore-Based Membranes. *Russ. Chem. Bull., Int. Ed.* Volume 61, 926-936.

[16] Agata Michalska. (2012) All-Solid-State Ion Selective and All-Solid-State Reference Electrodes. *Electroanalysis*. Volume 24, 1253 – 1265.

## **Chapter 2 : Au@Pt Core-Shell Nanoparticles Synthesis and Characteristics**

### **2-1- Introduction**

Nanoparticles are the basis of nanotechnology. Nanomaterials are being utilized in the vast area of biomedical applications as carriers for gene delivery, bio-detection of pathogens and hyperthermia treatment for tumor destruction diagnostics, and therapeutic areas to explore new drug targets or treatments [1].

Different types of bimetallic nanoparticles (BMNPs) are core-shell NPs, sub-cluster NPs, alloy NPs, and multi-shell NPs. Alloy NPs show different physical and structural properties than their original components. Nanoparticles are small in size, have relatively large surface-to-volume ratio, and most of them possess catalytic activity depending on their structural aspects. For this reason, they have attracted interest in the scientific community. Furthermore, their characteristics can be adjusted by changing their shape, size, and composition using synthetic methods [2].

Metal NPs can be produced in two different ways, by subdivision of bulk metals (a physical method) or by the growth of particles obtained from metal atoms, which are from molecular or ionic precursors (a chemical method) [2].

In our work, the core-shell category was chosen for Au@Pt nanoparticles preparation due to the large particle surface and simple synthesis procedure. Au nanoparticles as

template for Au@Pt core shell NPs preparation are beneficial due to their self-assembly, stability and the ability to prepare monodispersed colloids with a wide diameter range (1.5 to 100 nm) [3]. Because of Au@Pt NPs' long-term stability, simple and versatile synthetic approaches they are desirable [4].

Due to large surface area and high utilization efficiency, Pt and Pt based nanostructures exhibit unique catalytic activities. Considering the high costs of Pt, to reduce the consumption of Pt in Pt nanostructures their size and shape should be enhanced [5]. One of the ways to reach this goal is to combine Pt with other metal elements to form bi- or multi-metallic nanostructures [6].

In the case of combining Pt with Au, there are complex procedures proposed in the literature, which include at least two steps for the preparation of the core-shell nanostructures with a dendritic Pt shell, typically in high-temperature and high-pressure conditions. Consequently, a one-step synthesis of core-shell nanostructures with a high Pt surface area looks necessary. Another advantage of the one-step synthesis method is adjusting the Pt shell thicknesses around the core. In order to achieve a one-step synthesis procedure, a synthetic route for bimetallic Au@Pt nanocolloids with an Au core and a dendritic Pt shell can be employed. It can be done by performing a surfactant-assisted process with an ultrasonic irradiation treatment. This synthesis method permits the creation of monodispersed Au@Pt nanocolloids in various Pt precursor concentrations and accurate Pt shell thicknesses on the Au core [5]. Therefore, this method makes it possible to produce a set of uniform particles which can be applied in many applications.

One of the applications for these bimetallic nanoparticles is working as a transducer in an ion selective electrode. In our proposed ion-selective electrode, we used these particles as the solid contact on the electrode to detect the ammonium in human sweat. While we are introducing the Au@Pt core-shell nanoparticles synthesis and their properties in this chapter, the concept of ion-selective electrode and its characteristics will be discussed thoroughly in Chapter 3.

### **2-2- Other Published Works**

Here we overview some previously reported works on the use of other types of core-shell nanoparticles. In [7] Au@Pt core-shell particle was used for electrooxidation of carbon monoxide and methanol on platinum-overlayer-coated gold nanoparticles for monitoring the effects of film thickness. In that work, sodium citrate and  $\text{HAuCl}_4$  were used for core formation (Au) and Pt metal was utilized by electrochemical method to produce the shell (Pt) for the core-shell formation. In another work [8], Au@Pt core-shell nanoparticles with gold core and Pt shell were applied for the surface-enhanced Raman spectroscopy (SERS). In that paper, the core (Au) was formed by the reduction of  $\text{HAuCl}_4$  by sodium citrate. Likewise, the shell (Pt) was shaped by the reduction of  $\text{H}_2\text{PtCl}_6$  by ascorbic acid. In the paper [9], the electro-catalytic properties of platinum, overgrown on cubic, octahedral and spherical gold nanocrystals were investigated. In [10], Pt nanodots were formed on Au nanorods (NRs) by using a simple seed-mediated growth. Their density and distribution on the Au nanorod can be finely tuned by varying the reaction parameters. The core-shell exhibits a rod shape Au@Pt nanostructure [10, 11].

### **2-3- Au@Pt Core-Shell Nanoparticles**

This section discusses the Au@Pt core-shell nanoparticles synthesis and their characteristics for incorporating in an ammonium sensor. The different steps for the synthesis and characteristics of the Au@Pt core-shell nanoparticles will be discussed in the following sections.

#### **2-3-1- Material and Equipment**

Pluronic F-127 was purchased from Sigma-Aldrich. Ascorbic acid (AA) 99%, Hydrogen Tetrachloroaurate-(III) trihydrate ACS 99% ( $\text{HAuCl}_4 \cdot 3\text{H}_2\text{O}$ ), Dihydrogen Hexachloroplatinate (IV) hydrate 99.9% ( $\text{H}_2\text{PtCl}_6 \cdot x\text{H}_2\text{O}$ ) and Tetrahydrofuran 99% were purchased from Alfa Aesar. All other chemicals like acetone and deionized water were of analytical reagent grade. Deionized water was used to prepare the aqueous solutions.

Transmission electron microscope (TEM) images were acquired using a JEOL analytical transmission electron microscope equipped with an Oxford Energy-Dispersive X-ray (EDX) spectrometer. X-ray diffraction (XRD) data were collected by a coupled theta: 2-theta scan on a Rigaku Ultima-III diffractometer equipped with Copper X-ray tube with Ni beta filter, para-focusing optics, computer-controlled slits, and D/Tex Ultra 1D strip detector. In addition, an Ultrasonic bath was used during the experiments which is from Sper Scientific. Furthermore, vortex mixer from Scientific Industries were used during the experiments. A 500 mL glass vacuum container desiccator from Labconco also was used to dry out the particles.

### **2-3-2- Au@Pt Core-Shell Nanoparticles Synthesis**

In a typical synthesis of Au@Pt core-shell [5] (Pt/Au molar ratio = 1.0), 3.0 mL of 20 mM  $\text{H}_2\text{PtCl}_6$  solution and 3.0 mL of 20 mM  $\text{HAuCl}_4$  solution are mixed with 0.06 g of Pluronic F127 in a small beaker. Then we use magnetic stirring bar to stir the solution until the F127 is dissolved completely. In addition, 5.5 mL ascorbic acid 0.1 M is required in this synthesis. After that, both ascorbic acid and the mixture of Au and Pt in their beakers are placed in the mixture of ice and water in a container and are left to stir for 2 minutes. The ascorbic acid solution subsequently is added slowly to the Au and Pt mixture. Right after that the mixture is sonicated for 15 min. At the end, the solution is left to stir for 24 hours. After adding the Ascorbic acid, the reduction of Au ions preferentially occurs in a short time to produce Au cores. Afterward, the development of the Pt dendritic shell happens on the Au core. During the Pt dendritic formation, the Pluronic F127 plays an important role as a structural-directing agent [12].

After 24 hours of reaction, all the dissolved metal sources are completely formed. The color of the solution changes from yellow that contains Au and Pt ions and F127 (Figure 2-1.a) to red-brown after adding ascorbic acid (AA) solution and applying ultrasonic irradiation for 15 minutes (Figure 2-1.b). This indicates that only the Au species were preferentially reduced to Au nanoparticles. Finally, it changes to black (Figure 2-1.C) after 24 hours. The black color shows the formation of Au@Pt core-shell nanoparticles.

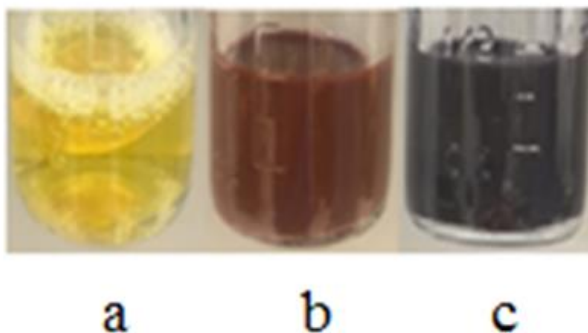


Figure 2-1: Au@Pt synthesis at different reaction times a) before adding ascorbic acid, b) after adding ascorbic acid and 15 minutes sonication, c) after 24 hours of stirring.

### 2-3-3- Washing and Drying the Synthesized Particles

Synthesized particle has some impurities that should be removed from Au@Pt resultant particles. Therefore, the product should be collected by centrifugation at 12000 revolutions per minute for 20 minutes. The residual pluronic F127 is removed by three consecutive washing and centrifugation cycles with acetone and water. Figure 2-2 shows the washing procedure of the synthesized particle that is done for three times. A glass vial of collected product is placed in a vacuum container desiccator and is left to dry at room temperature for 2 to 3 days [5]. The final dried particles are in the shape of black powder that can be dissolved in THF for ion selective electrode surface coating. The application procedure of these particles as a transducer layer in an ion selective electrode will be discussed in the next chapter.

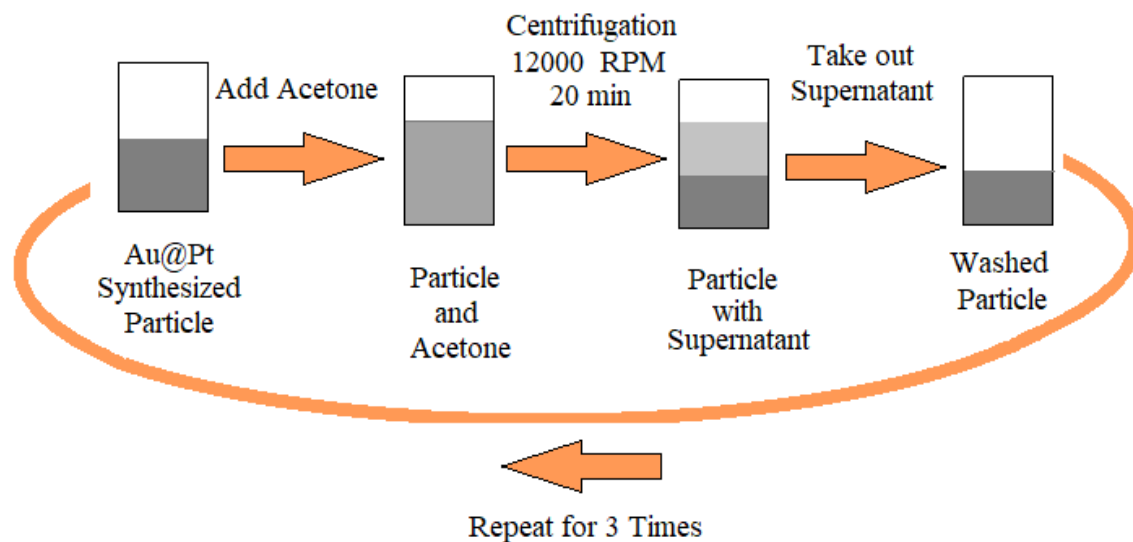


Figure 2-2: Washing procedure of the synthesized Au@Pt.

A variety of experimental techniques have been used to characterize and measure the properties of metal nanoparticles and nanoalloys such as mass spectroscopy, diffraction techniques, microscopy, X-ray spectroscopy, ion scattering, electrochemistry, and ion mobility measurements [13]. Among all of them we selected transmission electron microscopy (TEM) and energy dispersive X-ray spectroscopy (EDX) for Au@Pt nanoparticles identification. These two methods will be explained in the following.

Transmission electron microscopy works by passing the electrons through the sample. It generally requires the nanoparticles to be dispersed onto an electron-transparent substrate, such as a thin carbon-coated microgrid. TEM has the advantage of high contrast between the metal atoms and any passivating organic molecules or polymer [13]. The

TEM images of the Au@Pt synthesized particles are illustrated in Figure 2-3. The figure presents a cluster of particles and a single particle of synthesized Au@Pt. In addition, Figure 2-3 clearly demonstrates the formation of Pt dendrites around the Au core.

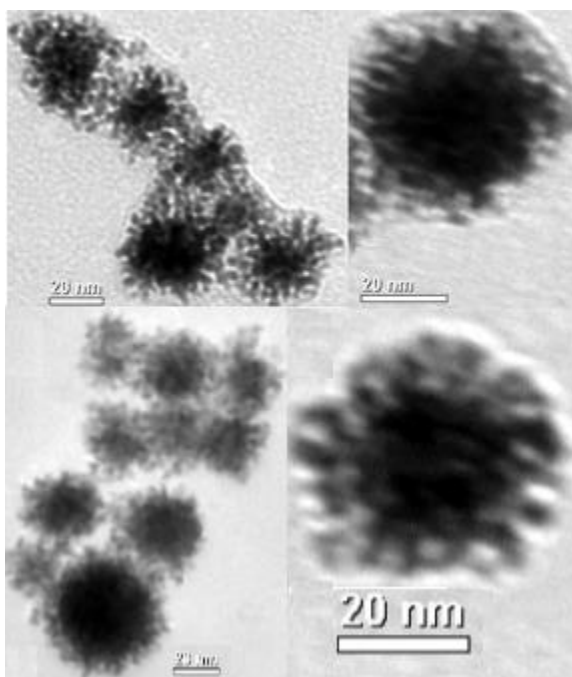


Figure 2-3: TEM images of Au@Pt core-shell NPs. (left) clusters of particles and (right) single particle.

Furthermore, in energy-disperse X-ray spectroscopy (EDX) an electron beam (10-20 keV) strikes the surface of a conducting sample, causing X-ray to be emitted with energies depending on the material under examination. The X-ray are generated in a region about  $2\ \mu\text{m}$  in depth. The electron beam is scanned across the sample, allowing an image of the

distribution of each element in the sample to be obtained. EDX is a high resolution (~ 1.5 nm lateral resolution) technique that allows spatially resolved determination of the chemical composition of individual metal nanoparticles [13].

Figure 2-4 displays the percentage of Pt and Au in the Au@Pt core-shell nanoparticles. The figure shows the synthesized particles composed of 41% Pt and 59% Au.

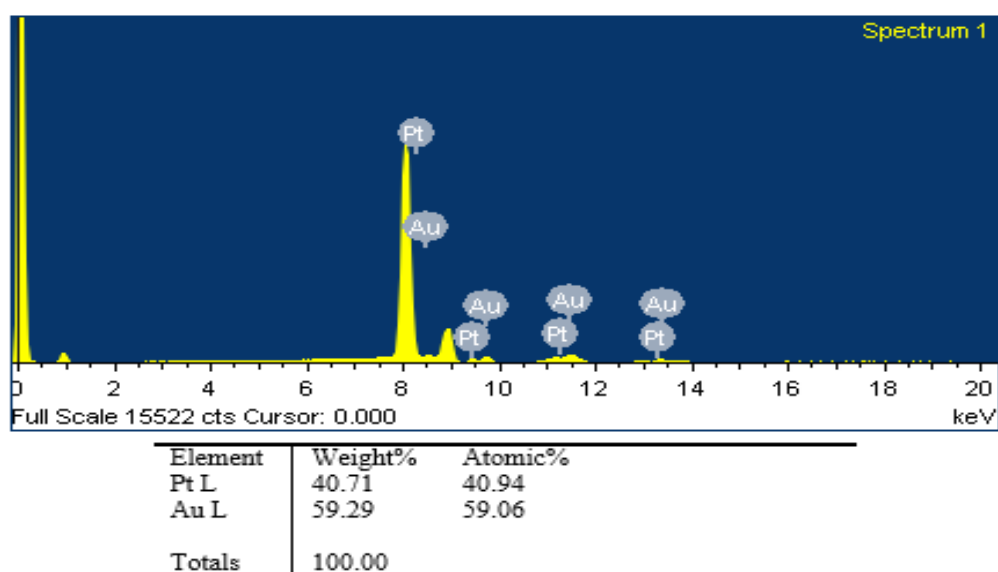


Figure 2-4: EDX results of Au@Pt particles and the percentage of each chemical in the Au@Pt nanoparticles.

According to the two performed tests, TEM and EDX, we observe that the synthesized particles are formed as core-shell nanoparticles in size of about 50 nm. Moreover, as the EDX test results show in Figure 2-4, the particles contain both Au and Pt components.

## 2-4- Conclusion

In this chapter we discussed the synthesis of Au@Pt core-shell nanoparticles and their characteristics. The method that we used for the particle synthesis is a new one-step procedure that utilizes the surfactant assisted process through an ultrasonication method. The synthesized particles, discussed in this chapter, comprise an Au core and a dendritic Pt shell. The synthesis does not include any complex procedures and it was done in the room temperature. The results of the TEM and EDX images indicate the formation of uniform sizes of about 50 nm for core-shell nanoparticles which combine Au and Pt elements. In the next chapter, we will explain the application of the Au@Pt core-shell nanoparticles in an ion selective electrode to detect the ammonium in human sweat.

## Reference

- [1] P. V. Asharani, Yi Lianwu, Zhiyuan Gong & Suresh Valiyaveetil. (2010) Comparison of the Toxicity of Silver, Gold and Platinum Nanoparticles in Developing Zebrafish Embryos. *Nanotoxicology*. 1–12. Doi: 10.3109/17435390.2010.489207.
- [2] Hamid Tayefi Nasrabadi, Elham Abbasi, Soodabeh Davaran, Mohammad Kouhi & Abolfazl Akbarzadeh, (2016) Bimetallic Nanoparticles: Preparation, Properties, and Biomedical Applications. *Artificial Cells, Nanomedicine, and Biotechnology*. Volume 44, 376-380. Doi: 10.3109/21691401.2014.953632.
- [3] Junfeng Zhai, Minghua Huang, Shaojun Dong. (2006) Electrochemical Designing of Au/Pt Core Shell Nanoparticles As nanostructured Catalyst with Tunable Activity for Oxygen Reduction. *Electroanalysis*. Volume 19, 506 – 509. Doi: 10.1002/Elan.200603728.
- [4] Mei-Yun Duan, Ren Liang, Na Tian, Yong-Jun Li, Edward S. Yeung. (2013) Self-Assembly of Au–Pt Core–Shell Nanoparticles for Effective Enhancement of Methanol Electrooxidation. *Electrochimica Acta*. Volume 87, 432–437. [Http://Dx.Doi.Org/10.1016/J.Electacta.2012.09.076](http://dx.doi.org/10.1016/j.electacta.2012.09.076).
- [5] Hamed Ataee-Esfahani, Liang Wang, Yoshihiro Nemoto, and Yusuke Yamauchi. (2010) Synthesis of Bimetallic Au@Pt Nanoparticles with Au Core and Nanostructured Pt Shell toward Highly Active Electrocatalysts. *Chem. Mater.* Volume 22, 6310–6318. Doi: 10.1021/Cm102074w.
- [6] Gui-Rong Zhang, Dan Zhao, Yuan-Yuan Feng, Bingsen Zhang, Dang Sheng Su, Gang Liu, And Bo-Qing Xu. (2012) Catalytic Pt-on-Au Nanostructures: Why Pt Becomes More Active on Smaller Au Particles. *Acs, Nano*. Volume. 6, 2226–2236.
- [7] Sachin Kumar and Shouzhong Zou. (2007) Electrooxidation of Carbon Monoxide and Methanol on Platinum-Overlayer-Coated Gold Nanoparticles: Effects of Film Thickness. *Langmuir*. Volume 23, 7365-7371.
- [8] Jian-Feng Li, Zhi-Lin Yang, Bin Ren, Guo-Kun Liu, Ping-Ping Fang, Yu-Xiong Jiang, De-Yin Wu, and Zhong-Qun Tian. (2006) Surface-Enhanced Raman Spectroscopy

Using Gold-Core Platinum-Shell Nanoparticle Film Electrodes: Toward a Versatile Vibrational Strategy for Electrochemical Interfaces. *Langmuir*. Volume 22, 10372-10379.

[9] Minkyu Min, Cheonghee Kim, Hyunjoo Lee. (2010) Electrocatalytic Properties of Platinum Overgrown on Various Shapes of Gold Nanocrystals. *Journal of Molecular Catalysis A: Chemical*. Volume 333, 6-10. Doi:10.1016/J. Molcata.2010.09.020.

[10] Lili Feng, Xiaochun Wu, Lirong Ren, Yanjuan Xiang, Weiwei He, Ke Zhang, Weiya Zhou, And Sishen Xie. (2008) Well-Controlled Synthesis of Au@Pt Nanostructures by Gold-Nanorodseeded Growth. *Chem. Eur. J.* 2008, 14, 9764 – 9771.

[11] Rajib Ghosh Chaudhuri and Santanu Paria. (2012) Core/Shell Nanoparticles: Classes, Properties, Synthesis Mechanisms, Characterization, and Applications. *Chem.Rev.* Volume 112, 2373-2433. Dx.Doi.Org/10.1021/Cr100449n.

[12] Liang Wang and Yusuke Yamauchi. (2009) Block Copolymer Mediated Synthesis of Dendritic Platinum Nanoparticles. *J. Am. Chem. Soc.* Volume 131, 9152–9153.

[13] Richard E. Plamer. (2012) Metal Nanoparticles and Nanoalloys. *Frontiers of Nanoscience Series Editor*. Volume 3. Edited by Roy L. Johnston, Jess Wilcoxon. Amsterdam Netherland.

## **Chapter 3 : Au@Pt Core-Shell Nanoparticles as Solid Contacts in Ion Selective Electrodes for Ammonium Detection**

### **3-1- Introduction**

A crucial component of an electrochemical ionic sensor is the ion-selective electrode. An ion-selective electrode has a membrane that transduces the chemical potential of a target ion into electric potential. Most ion-selective electrodes measure the electrochemical potential difference against a reference electrode in a near zero current or in an open circuit condition [1, 2].

Ion-selective electrodes (ISEs) are a common nondestructive monitoring tool for the ionic compositions. ISEs are normally in a cylindrical shape with a diameter of 8 mm to 12 mm and a length of 10 cm to 15 cm. They have a sensor membrane on one end and a connecting cable on the other end. Traditional ISEs also have an internal reference electrode and internal electrolyte. The internal aqueous solution holds the same ions the ISE membrane is selective with respect to it [3]. The problem with conventional ISEs is that they are relatively large due to the existence of the internal solution and the internal reference electrode. This affects their applicability in sample volumes below 1 mL, which are common in clinical analysis. Therefore, solid-contact ISEs (SC-ISEs), which do not have internal aqueous solutions, are increasingly being used in place of the traditional ISEs. Another advantage of the solid-contact ISEs is that they are maintenance-free and do not necessitate periodical replacement of the internal solution [3].

The regularly used materials to make solid contacts, transducer part of ion selective electrodes, are carbon, conductive polymers, and nanoparticles. Recently, there has been an increased interest in nanoscale materials. Nanomaterials are perfectly suited for sensors and biosensor applications because of their high surface area, high reactivity, ease of dispersion, and rapid fabrication [4]. Hence, we propose the use of Au@Pt core-shell nanoparticles as solid contact for ammonium ion selective electrode. The Au@Pt is synthesized according to the procedure explained in Chapter 2.

The membrane type that was used in our proposed ion selective electrodes is polymeric membrane. The most common ISEs are those with polymeric membranes containing ionophores. The selectivity of ionophores is the basis for the potentiometric selectivity of the respective ISEs [5]. The polymeric membrane we developed for our sensor contains PVC as the polymer, 2-Nitrophenyl octyl ether as the plasticizer, Sodium tetrakis [3,5-bis(trifluoromethyl)phenyl] borate (NaTFPB) as the ion-exchanger, and Nonactin as the ionophore to detect the ammonium in an analyte.

### **3-2- Other Published Works**

In paper [6] a potentiometric biosensor for creatinine detection was developed. The biosensor in that work is based on an ammonium ion-selective electrode with a PVC based ion selective membrane. The paper [7] proposed proton doped polyaniline (PANI) and copolymer of 2, 5-dimethoxyaniline and aniline (CPANI) as solid electrolyte to develop an all-solid-state  $\text{NH}_4^+$  ISE. In another work [8], an (vinyl chloride) ammonium ion-

selective electrode based on Nonactin is described, which focuses on 2-nitrophenyl octyl ether and trioctyl phosphate as solvent mediators for ammonium ion selective electrode.

In our work, we compare our proposed ISE with an ISE based on a Poly (3-Octylthiophene-2, 5-diyl), POT, solid contact. The POT-based ISE is another typical ion selective electrode in the literature. Furthermore, another ISE without the solid contact layer was prepared to monitor the effect of the proposed solid contact part on the response of the ammonium ISE. The latter electrode has only the membrane layers to detect the ammonium in the analyte. Therefore, we fabricated three electrodes for ammonium detection: First one with Au@Pt core-shell nanoparticle solid contact, second one with POT solid contact, and the third one without the solid contact. The membrane part of all electrodes was the same PVC-based membrane.

In the following, the experimental methods and the electrode preparation process will be discussed.

### **3-3- Experimental Methods**

#### **3-3-1- Chemicals and Apparatus**

Tetrahydrofuran 99%, lactic acid 85.0-90.0%, sodium hydroxide beads 99.99%, poly (3-Octylthiophene-2, 5-diyl) (POT), and magnesium chloride puratronic 99.999% were purchased from Alfa Aesar. Nonactin, poly vinyl chloride (PVC), and 2-nitrophenyl octyl ether (o-NPOE) were from Sigma-Aldrich. Potassium chloride, sodium chloride, acetic acid (glacial), hydrochloric acid chlorohydrique, standard ammonium solution (0.1 M)

and zinc chloride 98.0% were from Thermo fisher scientific. Sodium tetrakis [3, 5-bis (trifluoromethyl) phenyl]-borate (NaTFPB) were bought from Matrix Scientific, and calcium chloride dehydrate 99+% were from Acros Organics. All other chemicals like acetone and ethanol were of analytical-reagent grade.

The glassy carbon disc working electrode (3 mm in diameter) is from CH instruments. The Ag/AgCl reference electrode is from VWR. Fluke 45 Dual Display Multimeter and MATLAB software were used to measure and record the outputs of the ion selective electrodes. In order to adjust the pH of the solutions we used an YSI.inc pH meter with the model number of pH100. Two kinds of Ultrasonic bath were used during the experiments which are from Brandson and Sper Scientific. An ultrasonic microtip is from Misonix. Furthermore, a centrifuge from Eppendorf and a vortex mixer from Scientific Industries were used during the experiments. A 500 mL glass vacuum container desiccator from Labconco was also used to dry out the particles. Additionally, a typical flashlight was used to illuminate the proposed sensor for observing the effects of light changes on the sensor response during the measurements.

### **3-3-2- Ion Selective Membrane Preparation and ISE Fabrication**

The proposed ion selective membrane for ammonium detection is prepared with 59.25% plasticizer (o-NPOE), 1% of Nonactin, 0.3% NaTFPB, and 39.45% of PVC [9]. For the electrode preparation, the glassy carbon electrode is polished using 0.3  $\mu\text{m}$  sandpaper and rinsed with ethanol and water. Then 4 mg of Au@Pt particles, well suspended in 200  $\mu\text{L}$

of Tetrahydrofuran (THF) or 50  $\mu\text{L}$  of 0.25 mM POT [10] solution in THF, are added to the electrode surface. The electrode with the added layer is left to dry for 1 hour in the room temperature, then is coated with 120  $\mu\text{L}$  of membrane and dried in room temperature for another 48 hours [11]. The resultant electrodes should be conditioned in 0.1 M ammonium solution for 12 hours and dried for another 12 hours in the vacuum container desiccator in room temperature before further measurements are carried out. Figure 3-1 shows the scheme of the ion selective electrode (ISE) and various coated layers on the surface of glassy carbon disc electrode for ammonium detection.

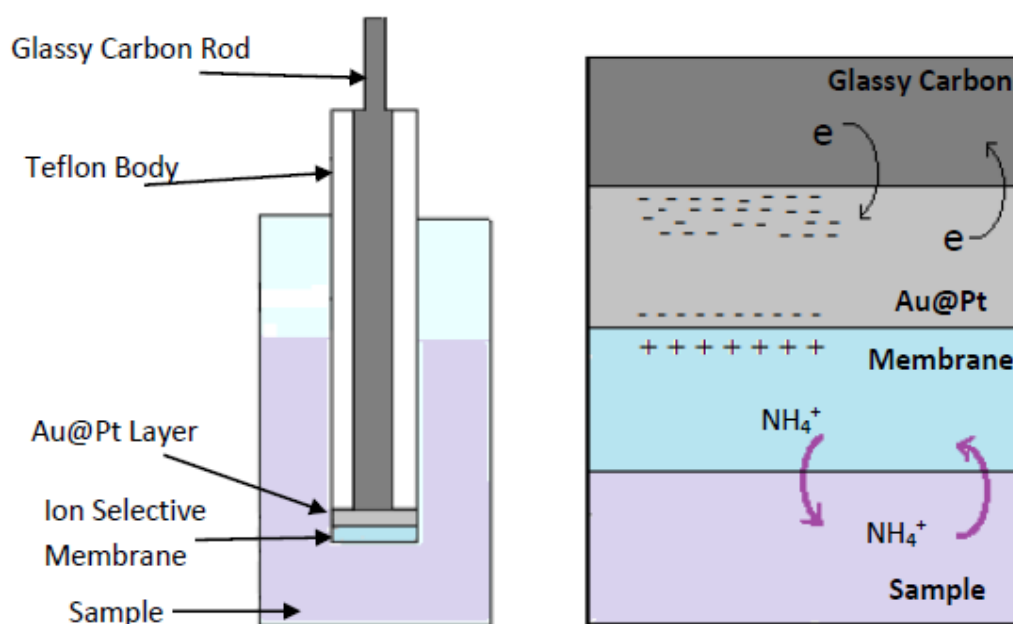


Figure 3-1: The scheme of the ion selective electrode (ISE) for ammonium detection as well as the illustration of the different layers of the ISE where Au@Pt nanoparticles are used as the solid contact.

In addition, various tests were performed for characterizing the electrode. Some of them, like selectivity and the artificial sweat tests require special samples. The preparation process of these samples will be explained in the following.

### **3-3-3- Artificial Sweat Preparation**

The artificial sweat is prepared according to the ISO 3160-2 standard. It contains 20 g/L sodium chloride, 17.5 g/L ammonium chloride, 5 g/L acetic acid, 15 g/L lactic acid that are mixed in DI water and its pH was adjusted to 4.7 by adding sodium hydroxide.

### **3-3-4- Selectivity Test Procedure and Potentiometric Selectivity Coefficient**

In order to calculate the selectivity coefficient of the ion selective electrode, the separate solution method (SSM) was employed. According to this method, the output potential of the ion selective electrode and the reference electrode are measured in two different solutions, the target ion and the interfering ion solutions [12].

To provide the sample for the selectivity test, six different 0.01 M solutions are prepared with various ions of  $\text{Na}^+$ ,  $\text{K}^+$ ,  $\text{NH}_4^+$ ,  $\text{Mg}^{2+}$ ,  $\text{Ca}^{2+}$ , and  $\text{Zn}^{2+}$ . For this reason, the required amount of NaCl, KCl,  $\text{MgCl}_2$ ,  $\text{CaCl}_2$ ,  $\text{ZnCl}_2$ , and  $\text{NH}_4\text{Cl}$  are added to DI water. Then each sample is examined by the proposed electrode for 2 minutes. The selectivity coefficient of each ion is calculated by using the potential result and the charge of the ions, as it is shown by the following equation:

$$\log K_{A,B}^{pot} = \frac{(E_B - E_A) z_A F}{RT \ln 10} + \left(1 - \frac{z_A}{z_B}\right) \log a_A \quad (3-1)$$

where A is the target ion ( $\text{NH}_4^+$ ), B is the interfering ion ( $\text{Na}^+$ ,  $\text{K}^+$ ,  $\text{Mg}^{2+}$ ,  $\text{Ca}^{2+}$ , and  $\text{Zn}^{2+}$ ),  $Z_A$  is the charge of the target ion ( $\text{NH}_4^+$ ) and is equal to 1,  $Z_B$  is the charge of the interfering ion ( $\text{Na}^+$ ,  $\text{K}^+$ ,  $\text{Mg}^{2+}$ ,  $\text{Ca}^{2+}$ , and  $\text{Zn}^{2+}$ ),  $a_A$  is activity coefficient equal to  $0.98 \cong 1$  [13]. The ratio the ratio  $RT/F$  is equal to 25.693 mV. Also,  $E_A$  is the measured potential of the target ion and  $E_B$  is from the interfering ion. In Equation (3-1), if  $Z_A = Z_B$  then  $\text{Log } K_{A,B} = (E_B - E_A)/59 \text{ mV}$ .

### 3-3-5- pH Adjustment

Since, the stability of electrode is tested for different pH values of the sample, various samples with different pH values of one concentration of ammonium solution were prepared during our experiments. The pH of the solution is measured by a pH meter and its pH is adjusted by Hydrochloric acid (HCl) and Sodium hydroxide (NaOH) solutions.

### 3-4- Test Results

The Au@Pt NP based ISE was mainly characterized in terms of calibration curve, response time, stability (water layer testing), and selectivity. To demonstrate the effects of Au@Pt NPs as solid contacts on sensing performance, an ISE using POT conductive polymer as the solid contact was fabricated and measured as a reference. The POT conductive polymer has been reported in literature as a solid contact for ISEs through casting on electrode surfaces. Additionally, an ISE without any solid contact but with

direct coating of ion selective membrane was fabricated and tested as a reference. Figure 3-2 represents the three electrode configurations for comparing their sensing performance.

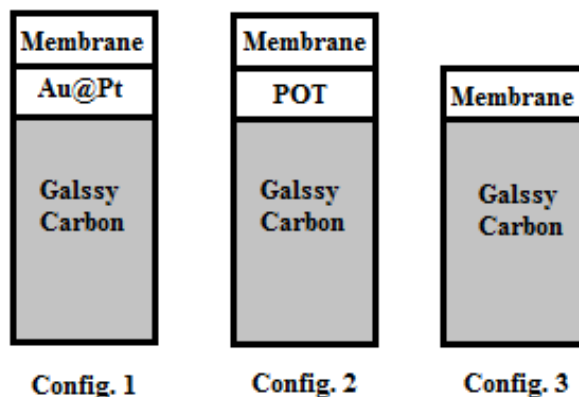


Figure 3-2: Three configurations of the ISE using different solid contact materials.

Figure 3-3 shows the obtained calibration curves of the ISEs using Au@Pt NPs, POT, and the electrode with the membrane part only. In Figure 3-3, the ISE using Au@Pt NPs has a slope at around 47 mV/decade and a detection range from  $10^{-5}$  M to  $10^{-1}$  M, while the ISE using POT has a slope at around 27 mV/decade and a detection range from  $10^{-5}$  M to  $10^{-2}$  M. The electrode without the solid contact has a slope of 10.3 mV/decade and a detection range of  $10^{-1}$  M to  $10^{-4}$  M.

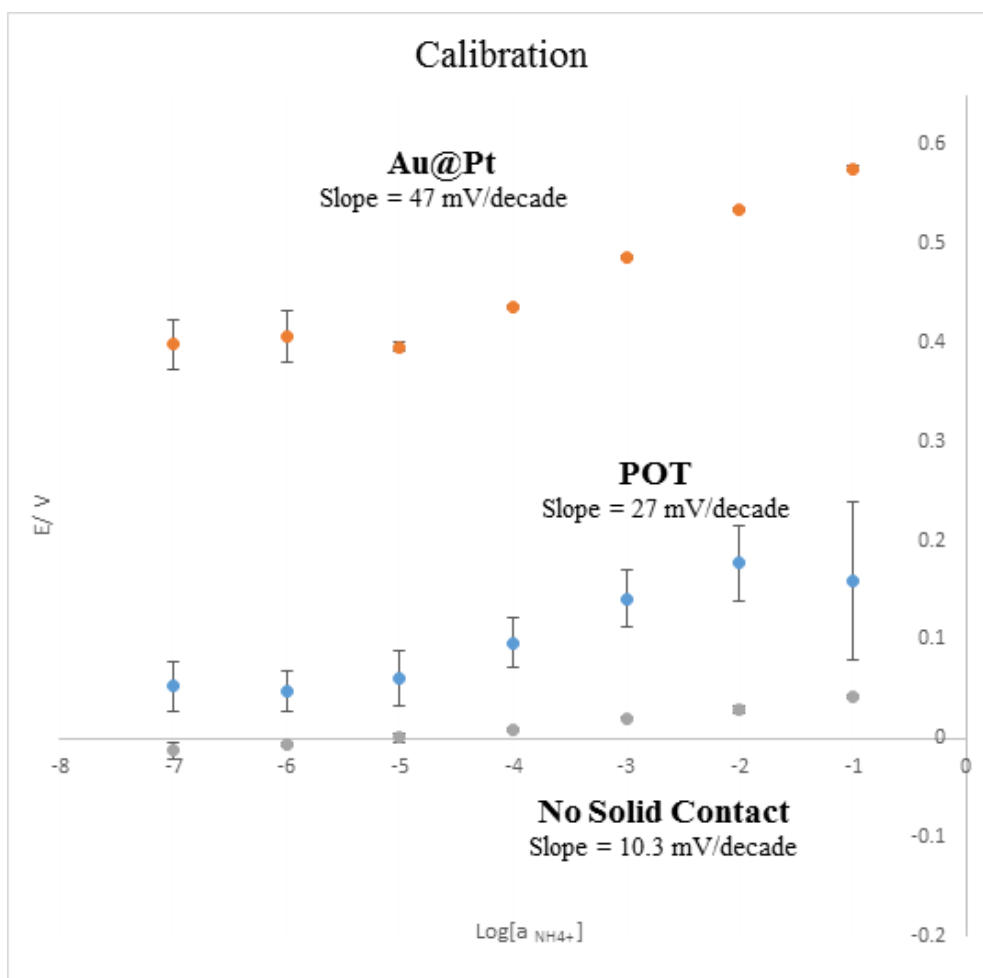


Figure 3-3: The calibration curves of the ISEs using Au@Pt nanoparticles, POT as solid contact, and the electrode without solid contact.

Figure 3-4 shows the responses of the three ISE configurations upon the changes of ammonium concentrations. The Au@Pt and POT solid contact ISEs show fast response times (2 ~ 4 seconds) on the concentration changes of ammonium. But the Au@Pt NP-based ISE presents a flatter or more stable response in each testing period for a fixed concentration, compared to the POT-based one. In contrast, the membrane only electrode

has a slow response time (more than 100 seconds) compared to the two other electrodes. Its measurements for various concentrations are also not flat and in the same level in forward and backward evaluations. It means, it is not accurate enough to detect the precise value of the ammonium in the sample.

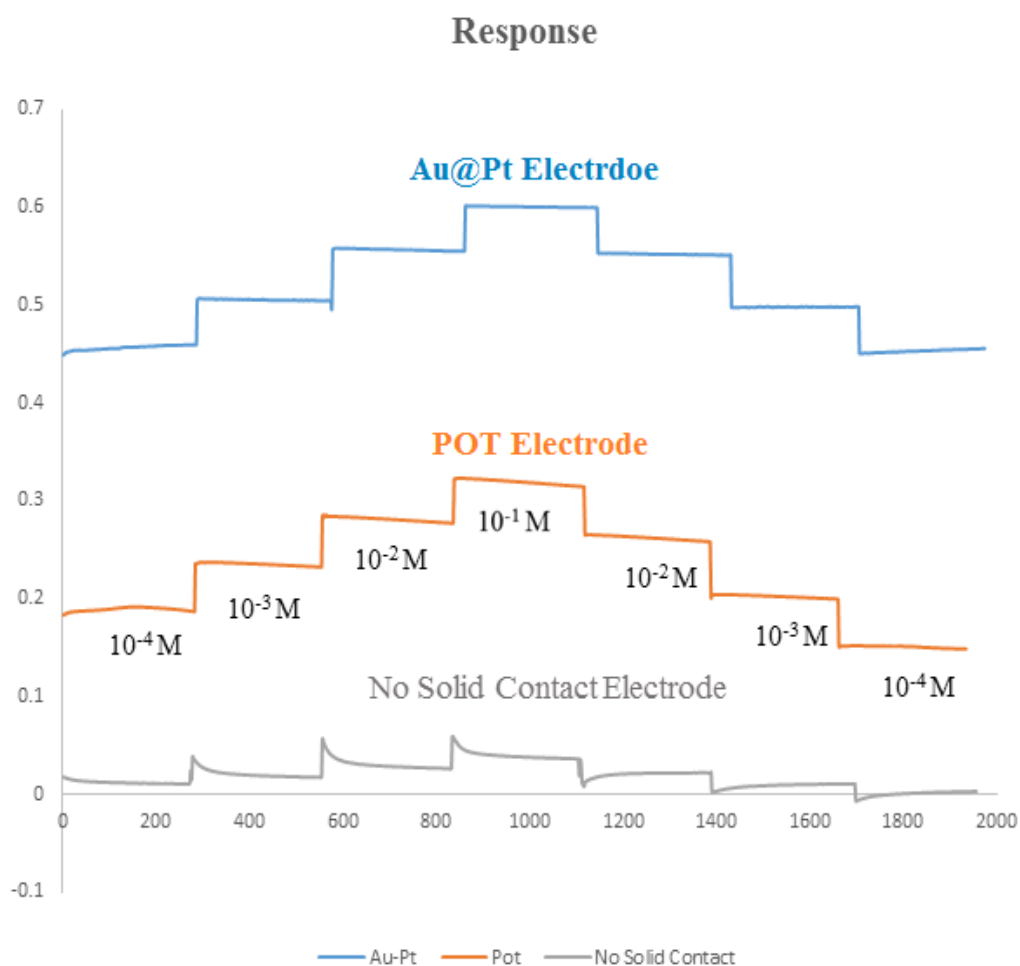


Figure 3-4: The electrode responses of the ISEs versus time with different ammonium concentrations for the three electrode configurations.

Figure 3-5 presents the water layer test results of the three ISEs. Water can penetrate through the ion-selective membrane into the solid contact layer or electrode surface, and thus cause the instability or drift of the electrode response. In the water layer testing, the electrode responses are measured in a  $10^{-1}$  M ammonium solution before and after dipping in a  $10^{-1}$  M sodium chloride solution. As shown in Figure 3-5, the Au@Pt NP-based ISE has an average drift of  $1.08 \times 10^{-6}$  V/second over 20 hours. The POT-based ISE shows an average drift of  $1.27 \times 10^{-6}$  V/second, but the output potential of the POT ISE is close to zero after a sharp voltage drift in a short time. The figure also shows the flat result for the non-solid contact ISE that presents a potential value close to zero.

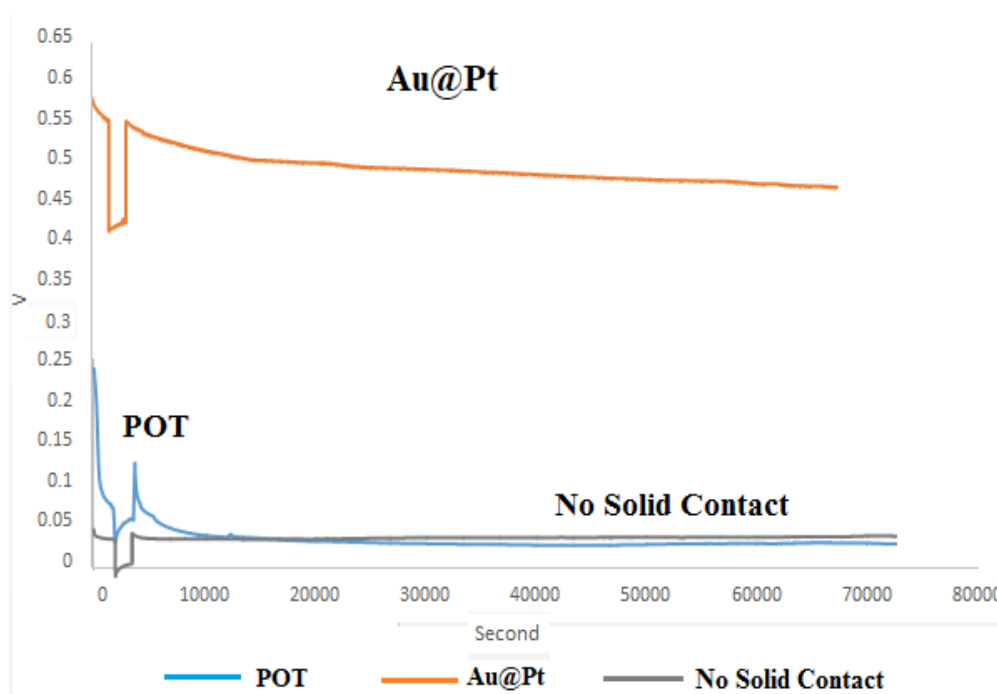


Figure 3-5: The water layer tests on the ISEs using Au@Pt nanoparticles and POT as solid contacts and the electrode with membrane only (no solid contact).

Table 3-1 summarizes the sensing performance of the ISEs in the three configurations including their calibration slopes, response characteristics, the electrode response drift in water layer tests, and their selectivity against common ions such as  $\text{Na}^+$ ,  $\text{K}^+$ ,  $\text{Ca}^{2+}$ ,  $\text{Mg}^{2+}$ , and  $\text{Zn}^{2+}$ . Notably, for the ISE without any solid contact, its sensing performance is not comparable to the ISEs in the other two configurations. Through the comparison with the POT-based ISE, it can be seen that the Au@Pt NP-based ISE achieved a better sensing performance.

Table 3-1: Sensing performance of the three ISE configurations

Electrodes	Calibration	Response	Water Layer	Selectivity Coefficient	
GC/Au@Pt/membrane (Config.1)	~ 47 mV/decade	Fast and flat for each test period	~ $1.08 \times 10^{-6}$ V/s	$\text{Na}^+$	-2.25
				$\text{K}^+$	-0.89
				$\text{Ca}^{2+}$	-4.04
				$\text{Mg}^{2+}$	-4.03
				$\text{Zn}^{2+}$	-3.97
GC/POT/membrane (Config.2)	~ 27 mV/decade	Fast but not flat for each test period	~ $1.27 \times 10^{-6}$ V/s	$\text{Na}^+$	-2.23
				$\text{K}^+$	-0.83
				$\text{Ca}^{2+}$	-4.28
				$\text{Mg}^{2+}$	-4.47
				$\text{Zn}^{2+}$	-4.32
GC/membrane (Config.3)	~ 10 mV/decade	Not flat for each test period	Significant drift	$\text{Na}^+$	-0.73
				$\text{K}^+$	-0.23
				$\text{Ca}^{2+}$	-1.80
				$\text{Mg}^{2+}$	-1.93
				$\text{Zn}^{2+}$	-1.69

Table 3-2 shows the comparison between some published works and the proposed Au@Pt NP-based ISE. With respect to the limit of detection, the calibration slope, the linear range, and the water layer drift, the comparison data show that the sensing performance of the Au@Pt NP-based ISE is in the range of other reported results.

Table 3-2: Sensing performance comparison with other reported electrodes.

<b>Solid Contact of ISE</b>	<b>Detection Limit (M)</b>	<b>Slope (mV/Decade)</b>	<b>Linear Range (M)</b>	<b>Drift (Reference)</b>
Au@Pt	$10^{-5.0}$	47	$10^{-5} - 10^{-1}$	$1.08 \times 10^{-6}$ V/s (this work)
IPG	$10^{-5.2}$	57.2	$10^{-5} - 10^{-2}$	$8.6 \times 10^{-6}$ V/s [14]
CNT	$10^{-5.5}$	58.4	$10^{-5.5} - 10^{-2.5}$	$1.7 \times 10^{-5}$ V/s [15]
Graphene/GC	$10^{-5.0}$	59.2	$10^{-4.5} - 10^{-1}$	$1.2 \times 10^{-5}$ V/s [16]
Fullerene	$10^{-5.0}$	55	$10^{-5} - 10^{-2}$	N/A [17]
CIM Carbon	$10^{-5.6}$	59.5	$10^{-5.2} - 10^{-1}$	$0.36 \times 10^{-3}$ $\mu$ V/s [18]
Porous Carbon	$10^{-5.7}$	57.8	$10^{-5} - 10^{-1}$	$4.1 \times 10^{-3}$ $\mu$ V/s [19]

Figure 3-6 shows the effect of pH values on the ISE response. In the pH test, the  $10^{-3}$  M ammonium samples were prepared with different pHs from 2 ~ 12. It can be seen that the ISE response is relatively stable for the pH range from 2 to 8, but significantly drops at higher pHs (10-12).

Figure 3-7 presents the effect of light on the electrode response. The ISE was tested with a  $10^{-3}$  M ammonium sample by periodically turning on/off light (flashlight, 30 W) directly pointed to the ISE in the dark. As shown in Figure 3-7, the ISE response does not show any significant fluctuation caused by light.

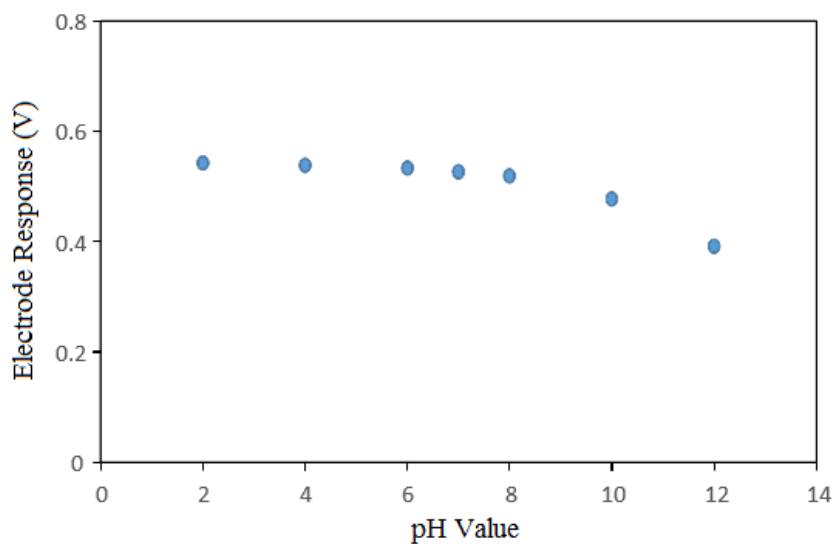


Figure 3-6: Effect of pH values on the response of the proposed electrode.

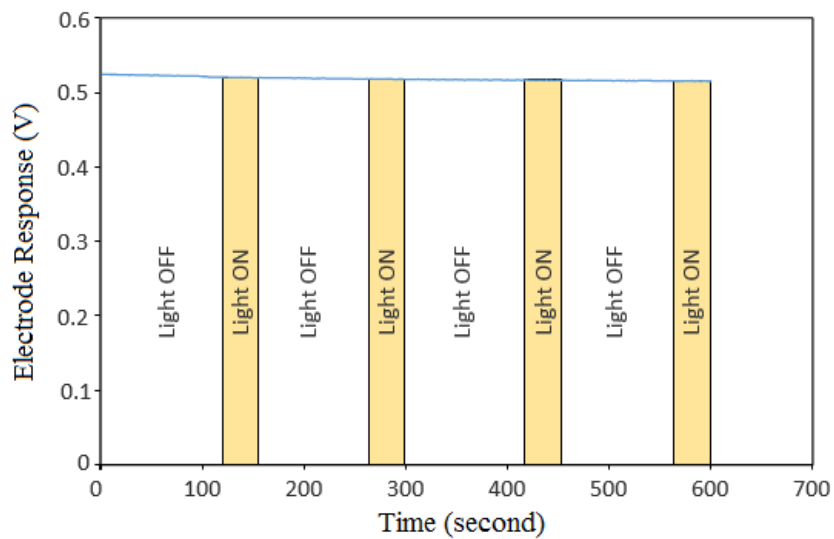


Figure 3-7: Effect of light on the response of the proposed electrode.

To investigate the fabrication repeatability and the testing stability of the proposed Au@Pt NP-based ISE, three ISEs were fabricated with the same procedure and their calibration curves were tested over ten days (ISEs were stored in room temperature to dry before each calibration test). Figure 3-8 shows the calibration curves of the three ISEs tested in the same day. It is observed that their calibration curves have some offsets from each other which could be caused by errors involved in the fabrication process, but these ISEs did present very similar calibration slopes, the linear ranges, and the limit of detections. The inner set in Figure 3-8 illustrates a presentative shift of the calibration curve over ten days by testing one individual ISE. The measurement drift over time was also observed for the other ISEs as reported in literatures. Although the drift is small from Day 5 to Day 10 and the ISE's output electrical potential is reasonably stable for this period, there are still some drifts. To overcome these effects in measurement, the conventional sensor calibration strategy (calibrating sensors right before measuring a sample) is suggested.

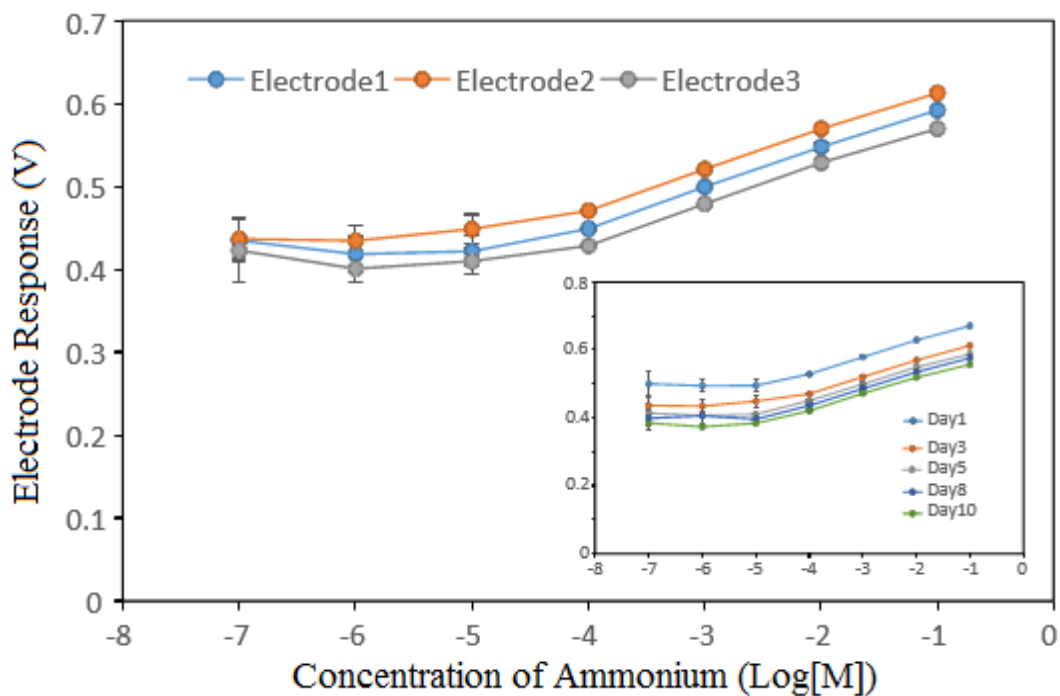


Figure 3-8: The repeatability testing results of three fabricated electrodes through measuring and comparing their calibration curves. The inset shows the drift of an individual electrode in the course of time.

Figure 3-9 shows the stability of the three fabricated ISEs over ten days by measuring  $10^{-3}$  M ammonium while adopting the calibration strategy for each measurement. In the test, each ISE was calibrated first using  $10^{-2}$  M and  $10^{-4}$  M ammonium and then applied to measure  $10^{-3}$  M ammonium. It should be noted that the short-term response of each ISE is relatively stable (e.g. for each 10 ~ 20 min), because the water-layer drift is at  $1.08 \times 10^{-6}$  V/second.

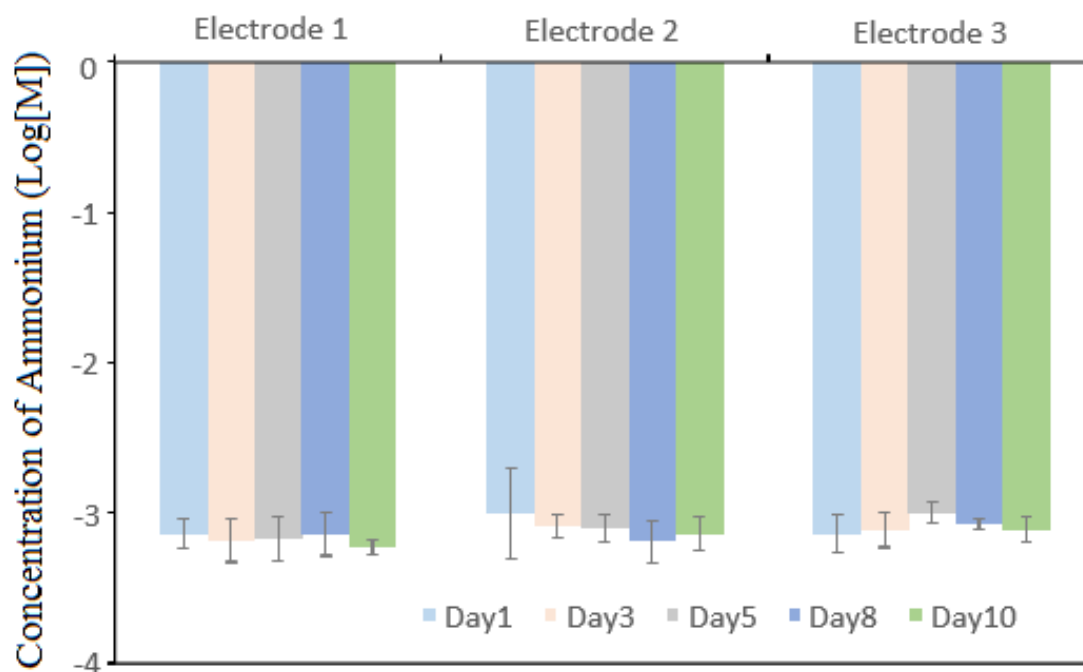


Figure 3-9: The measurement stability of three fabricated electrodes using the two-point calibration strategy for each measurement.

Figure 3-10 shows a potential application of the proposed ISE, the ISE response on the testing of DI water, artificial sweat without ammonium, and artificial sweat containing ammonium. The ISE output presented a clear electrical potential jump when the solution under the test was changed from DI water to artificial sweat without ammonium. This jump should be related to the interference from sodium ions in the artificial sweat without ammonium. The sodium ions exist, because of the utilized sodium chloride in the artificial sweat and the sodium hydroxide which was added to the sample to adjust the pH to 4.7 (according to the ISO 3160-2 standard). When the testing solution was changed from artificial sweat without ammonium to artificial sweat containing ammonium, the ISE

presented a higher potential jump which corresponds to the ammonium in the artificial sweat. The ISE presented a good testing repeatability as the testing solution was switched back to the artificial sweat without ammonium and then DI water. The results in Figure 3-10 clearly indicate that the Au@Pt NP-based ISE is capable of properly distinguishing the samples with ammonium from those which have none in a complex sample matrix.

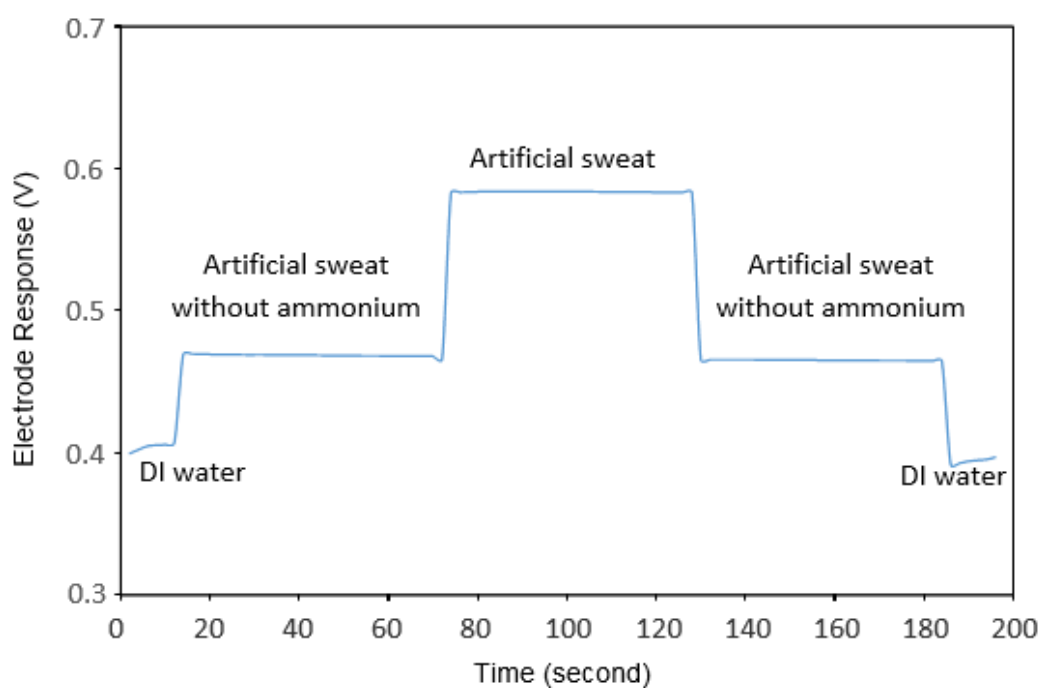


Figure 3-10: A representative real-world measurement of the artificial sweat using the proposed electrode. DI water and artificial sweat without ammonium were also measured as references.

### 3-5- Conclusion

In this chapter an ISE for ammonium detection was proposed and characterized. The developed ISE comprises of Au@Pt core-shell nanoparticles as solid contact and the PVC-based membrane for ammonium detection on top of the solid contact. As the tests results in this chapter show, the proposed electrode is in the appropriate range of the other published works. The sensor displayed fast response and acceptable selectivity, even in the presence of other ions. In addition, the sensor is insensitive to light changing and is stable in the 2-8 pH range. These characteristics validate the sensor's applicability to properly determine the ammonium level in an unprotected environment. Moreover, the sensor measurements are reliable in a long duration of time, as the results presented in Figure 3-9 demonstrate insignificant changes in an interval of 10 days. In spite of all the afore-mentioned advantages, though, the ISE needs to be more resistive to water layer formation in different layers of the solid contact and the membrane.

## Reference

- [1] Tanushree Ghosh, Hyun-Joong Chung, and Jana Rieger. (2017) All-Solid-State Sodium-Selective Electrode with A Solid Contact of Chitosan/Prussian Blue Nanocomposite. *Sensors*. Volume 17, 2536. Doi: 10.3390/S17112536.
- [2] Johan Bobacka, Ari Ivaska, and Andrzej Lewenstam. (2008) Potentiometric Ion Sensors. *Chem. Rev.* Volume 108, 329–351.
- [3] V. V. Timofeev, M. B. Levin, A. A. Starikova, M. A. Trofimov, S. M. Korneev, and K. N. Mikhelson. (2018) Solid-Contact Ion-Selective Electrodes with Copper Hexacyanoferrate in the Transducer Layer. *Elektrokhimiya*. Volume 54, 458–466. Doi: 10.1134/S1023193518040080.
- [4] Beata Paczosa-Bator, Leszek Cabaj, Robert Piecha and Krzysztof Skupie. (2012) Platinum Nanoparticles Intermediate Layer in Solid-State Selective Electrodes. *Analyst*. Volume 137, 5272. Doi: 10.1039/C2an35933b.
- [5] Konstantin N. Mikhelson. (2013) *Ion-Selective Electrodes*. Springer-Verlag Berlin Heidelberg. Volume 81. DOI:10.1007/978-3-642-36886-8
- [6] Anna Radomska, Ewa Bodenzac, Stanisław Głab, Robert Koncki. (2004) Creatinine Biosensor Based on Ammonium Ion Selective Electrode and Its Application in Flow-Injection Analysis. *Talanta*. Volume 6, 4603–608. Doi:10.1016/J. Talanta.2004.03.033.
- [7] Yuanfeng Huang, Jun Li, Tianya Yin, Jianjun Jia, Qian Ding, Hao Zheng, Chen-Tung Arthur Chen, Ying Ye. (2015) A Novel All-Solid-State Ammonium Electrode with Polyaniline and Copolymer of Aniline/2, 5-Dimethoxyaniline as Transducers. *Journal of Electroanalytical Chemistry*. Volume 741, 87-92.
- [8] M. S. Ghauri and J. D. R. Thomas. (1994) Poly(Vinyl Chloride) Type Ammonium Ion-Selective Electrodes Based on Nonactin: Solvent Mediator Effects. *Analytical Proceedings Including Analytical Communications*. Volume 31.
- [9] Ding L, Ding J, B Ding, Qin W (2017) Solid-Contact Potentiometric Sensor for the Determination of Total Ammonia Nitrogen in Seawater. *Int. J. Electrochem. Sci*. Doi: 10.20964/2017.04.01.

- [10] Jolanda Sutter, Erno Lindner, Robert E. Gyurcsanyi, Erno Pretsch. (2004) a polypyrrole-based solid-contact  $Pb^{2+}$ -selective PVC-membrane electrode with a nanomolar detection limit. *Anal Bioanal Chem.* Volume 380, 7–14. DOI 10.1007/s00216-004-2737-4
- [11] Paczosa-Bator B, Cabaj L, Piecha R, Skupień K (2012) Platinum Nanoparticles Intermediate Layer in Solid-State Selective Electrodes. *Analyst.* Doi: 10.1039/C2an35933b.
- [12] Yoshio Umezawa, Philippe Bühlmann, Kayoko Umezawa, Koji Tohda, and Shigeru Amemiya. (2000) Potentiometric Selectivity Coefficients of Ion-Selective Electrodes. *Pure Appl. Chem.* Volume 72, 1851–2082.
- [13] R. E. Verrall (1975) Determination of Activity Coefficients for Ammonium Chloride at 25°C. *Journal of Solution Chemistry.* Volume 4, 319-329.
- [14] He Q (2017) the Development of Carbon Nanomaterials Enhanced Potassium Sensor and Glucose Sensor for Applications in Wearable Sweat-Based Sensing. Dissertation, Iowa State University.
- [15] Crespo Ga, Macho S, Rius Fx (2008) Ion-Selective Electrodes Using Carbon Nanotubes as Ion-To-Electron Transducers. *Anal Chem.* Doi: 10.1021/Ac071156l.
- [16] Li F, Ye J, Zhou M, Gan S, Zhang Q, Han D, Niu L (2012) All-Solid-State Potassium-Selective Electrode Using Graphene as the Solid Contact. *Analyst.* Doi: 10.1039/C1an15705a.
- [17] Fouskaki M, Chaniotakis N (2008) Fullerene-Based Electrochemical Buffer Layer for Ion-Selective Electrodes. *Analyst.* Doi: 10.1039/B719759d.
- [18] Hu J, Zou X. U, Stein A, Bühlmann P (2014) Ion-Selective Electrodes with Colloid-Imprinted Mesoporous Carbon as Solid Contact. *Anal. Chem.* Doi: 10.1021/Ac501633r.

[19] Ye J, Li F, Gan S, Jiang Y, An Q, Zhang Q, Niu L (2015) Using Sp<sup>2</sup>-C Dominant Porous Carbon Sub-Micrometer Spheres as Solid Transducers in Ion-Selective Electrodes. *Electrochem. Commun.* <https://doi.org/10.1016/j.elecom.2014.10.014>.

## **Chapter 4 : Conclusion**

### **4-1- Conclusion**

In this work, Au@Pt core-shell NPs were synthesized and used as solid contacts in an ion selective electrode for detection of ammonium ions. Observations showed a shell layer of Pt particles around the Au cores. The Au@Pt NPs are easy and fast to synthesize in room temperature. The synthesis process of the particles were done in one step and in room temperature. It is straightforward compared to the other methods in the literature. The resultant particles have uniform core-shell shapes.

The Au@Pt NP-based ISE was prepared by a PVC and ionophore-based membrane for ammonium detection. Ammonium detection is important for monitoring and diagnosis of some kidney and liver abnormalities. When urea that achieved from ammonia in the liver cannot leave the body, because of kidney or liver failure, ammonia remains in the human body and it causes several problems like confusion, extreme tiredness, and in some cases coma or even death.

The ISE presented a reasonable calibration slope, a fast response time, and acceptable stability in water layer testing. In addition, the ISE shows a relatively stable response for an ammonium sample with a pH range of 2 to 8 and is insensitive to light disturbance. The ISE was applied to test artificial sweat and achieved a reasonable response in a complex sample matrix. It is believed that Au@Pt NPs could be mixed with certain

solvents and printed on flexible surfaces to build arrays of ISEs or other sensors for wearable or point-of-care applications.

#### **4-2- Future Work**

Future work will focus on the surface modification of Au@Pt nanoparticles to make them hydrophobic while keeping their conductive properties, which may further help reduce the water layer in ion selective electrodes by using them as solid contacts and enhance ion selective electrode's long-term stability. Moreover, implementing the proposed ion selective electrode on flexible materials can be a future research direction in our work. That makes the proposed ion selective electrode suitable as a part of a wearable sensor for in situ detection of ammonium in perspiration.

To prepare a wearable sensor, the minimum level of the sample which it is needed for detection of the target ion should be measured precisely. Reducing the minimum level of sample can make the sensor applicable and more sensitive to small volume of the sweat on the human body.